Hindawi
Mathematical Problems in Engineering
Volume 2021, Article ID 8353844, 10 pages
https://doi.org/10.1155/2021/8353844

Research Article

Effects of Ship Propulsion Shafting Alignment on Whirling Vibration and Bearing Temperature Response

Junsong Lei,[1] **Ruiping Zhou**,[1] **Hao Chen**,[1] **Guobing Huang**,[1] **Yakun Gao**,[2] **and Qingcao Yang**[3]

[1]*School of Energy and Power Engineering, Wuhan University of Technology, Wuhan 430063, China*
[2]*Wuchang Shipbuilding Industry Group Co., Ltd., Wuhan 430000, China*
[3]*Naval University of Engineering, Wuhan 430032, China*

Correspondence should be addressed to Junsong Lei; hbljs0221@163.com

Received 5 June 2021; Accepted 11 September 2021; Published 27 September 2021

Academic Editor: Rossana Dimitri

Ship's propulsion shafting is one of the main sources of ship vibration and noise. The shafting, whirling vibrations, and alignment are important factors that affect the comfort, stability, and reliability during a ship's navigation. However, the mechanism of the interacting of the both factors is not fully revealed. In this paper, the effect of shafting alignment on whirling vibration and the bearing temperature response is studied by experiment. The test scheme is designed reasonably according to the theoretical analysis. The results show that the horizontal component of the shafting whirling vibration can be effectively reduced by adjusting the shafting alignment state while the vertical component is not. The shafting axis balancing position (SABP) slightly moves upward in high speed, which should be considered in the dynamic alignment design of the shafting, especially for the high-speed shafting. Little ABSB (the angle between the shafting centre line and the No. 1 bearing centre line) is beneficial to the stable operation of shafting, while appropriately increasing the ABSB and bearing load is beneficial to reducing the shafting whirling vibration. By balancing the relationship between bearing load and ABSB, the performance of whirling vibration and bearing temperature response can be optimized.

1. Introduction

As an important part of the ship power plant, propulsion shafting is one of the main excitation sources of ship vibration and noise. Nowadays, the improvement of the comfort requirements makes the vibration and noise reduction works attract much attention in the field of ship construction. It is especially important for super large luxury cruise ships and other passenger ships. When the ship is sailing, shafting alignment and the bearing supporting condition will be greatly affected by the dynamic factors such as hull deflection and hydrodynamic which will greatly affect the shafting vibration performance. However, the mechanism of the interacting of these factors is not fully revealed. The effect of dynamic factors such as dynamic shafting alignment and vibration performance has been paid increasing attention.

Massive research work has been carried on to propulsion shafting alignment and whirling vibration. The study on shafting alignment mainly focused on factors such as hull deformation and bearing supporting performance to improve the reliability of shafting operation [1–5]. The investigation on shafting whirling vibration is relatively diverse. The effects of cracked shaft, gyroscopic effect, and material properties on the shafting whirling vibration and the latest measurement methods are analysed [6–10]. Many researchers also made their works combining the shafting alignment and whirling vibration together. Xu et al. developed a novel model of a hydraulic turbine generator system considering the hydro-mechanical-electrical factors

[11]. Huang et al. proposed a nonlinear numerical model to investigate the coupled transverse-torsional vibrations when shafting rotating. They found that the natural frequencies are little affected by speed, load, and so on [12, 13]. Wang and Jiang derived and solved the differential equations of the dual-rotor system with unbalance-misalignment coupling faults numerically and verified the dynamic model by experiment [14]. Hujare and Karnik presented the effect of parallel misalignment of *A*l shaft rotor on its vibration response by experimental and numerical analysis. They found that the 1X, 2X, and 3X characteristic frequencies have maximum values of vibration amplitude [15]. Tuckmantel and Cavalca established the shaft misalignment model and got the harmonic components rising due to misalignment and verified it by test. They proposed the effect of coupling angular misalignment on the harmonic components of vibration and the orbit shapes of the shafting [16]. Sawalhi et al. adapted finite element simulations and designed experiments to study the method of vibration modelling and diagnosis of misalignment beyond traditional approaches [17]. However, these works are mainly focused on the field of fault diagnosis. Li et al. found that the vibration characteristics of the shafting with angle misalignment have strong nonlinearity [18]. Patel and Darpe investigated the vibration response of a rotor with a misaligned flange by using the method of finite element analysis and experiment. Their research showed that the misaligned flange has a remarkable effect on the torsion vibration and transverse vibration of the shafting system [19]. Yang Guodong investigated the influence of alignment on the shafting vibration by analysing the bearing lubrication characteristics [20]. Lai et al. optimized the alignment state and inherent vibration characteristics of a motor drive propulsion shafting by adjusting the bearing offset and presented the optimization weight coefficient [21, 22]. Yang-Yang and Jun found that adopting the shafting alignment scheme according to the bearing load can suppress the vibration transmission at some peak frequency points [23]. Although these studies have drawn some related conclusions, the influence law of marine propulsion shafting alignment on shafting vibration has not been revealed.

According to the aforementioned research, comprehensive studies on the combination of shafting alignment and vibration are seldom used in ship design and construction production practically. In this work, the finite element method (FEM) model of the test rig shafting designed by Wuhan University of Technology (WUT) is built. The shafting alignment and whirling vibration characteristic was analysed by FEM. Combined with the calculation results, the initial alignment state of the shafting was determined by experiments. Then, a reasonable experimental analysis scheme is designed, and the effect of alignment state of shafting on whirling vibration response is investigated. The results show that the whirling vibration can be effectively reduced by adjusting the shafting alignment state. The displacement of the SABP should be considered during shafting alignment design, especially for the high-speed shafting. The reduction of ABSB decreases the whirling vibration.

The innovation of this work comes in 3 aspects: (1) the effect of shafting alignment on vibration is studied experimentally from the view of the actual ship shafting installation; (2) some influence laws of shafting alignment on whirling vibration are revealed from the actual shafting response phenomenon, and (3) it is founded that the shafting whirling vibration can be effectively reduced by adjusting the shafting state reasonably.

2. Shafting Models

In this section, the structure and parameters of the test rig for shafting alignment and whirling vibration investigation designed by WUT are introduced. The shafting is supported by three bearings and driven by an electric motor, which will reduce the influence of the driving element. The actual ship propulsion shafting is simulated by the weight disk on the shaft according to the theory analysis. The actual structure of the test rig is shown in Figure 1, and the main parameters of the shafting are listed in Table 1.

3. Theoretical Basis and Experiment Design

In this section, the shafting alignment and whirling vibration characteristic were analysed by FEM. Combined with the analysis results, the shafting initial alignment state was determined by experiments. Then, a reasonable experimental analysis scheme is designed.

3.1. Shafting Alignment. The shafting model of the test rig was established using beam element by the finite element method. Each bearing was simplified into two equivalent springs in horizontal and vertical directions with an isotropic stiffness value of 5×10^9 N/m [21]. The shear vector $\{\mathbf{Q}\}^e$ and deformation vector $\{\delta\}^e$ of each element are as follows:

$$\left\{ \begin{array}{c} \{\mathbf{Q}\}^e = \left(\mathbf{Q}_i^e, \mathbf{Q}_j^e\right)^T = \left(\mathbf{T}_i, \mathbf{M}_i, \mathbf{T}_j, \mathbf{M}_j\right)^T \\ \{\boldsymbol{\delta}\}^e = \left(\boldsymbol{\delta}_i^e, \boldsymbol{\delta}_j^e\right)^T = \left(\mathbf{y}_i, \boldsymbol{\theta}_i, \mathbf{y}_j, \boldsymbol{\theta}_j\right)^T \end{array} \right\}, \quad (1)$$

where $\mathbf{T}$, $\mathbf{M}$, $\mathbf{Y}$, and θ are the shear, bending moment, vertical displacement, and the angle around the axis of node i and j, respectively. The relationship between force and deformation is shown in equation (2). The stiffness matrix is as shown in formula (3).

Figure 1: Actual structure diagram of the test rig.

Table 1: Main parameters of the test rig.

Parts	Parameters	Value
Electromotor	Rated power	5 kW
	Speed	0~2500 r/min
	Rated torque	15 N·m
Shaft	Length	2020 mm
	Diameter	35 mm
Weight disc		
1	Weight	5 kg
2		25 kg

$$\{\mathbf{Q}\}^e = \mathbf{K}_e \boldsymbol{\delta}_e, \tag{2}$$

$$\mathbf{K}_e = \frac{EI}{1+\phi}\begin{bmatrix} \frac{12}{l^3} & \frac{6}{l^2} & -\frac{12}{l^3} & \frac{6}{l^2} \\ \frac{6}{l^2} & \frac{4+\phi}{l} & -\frac{6}{l^2} & \frac{2-\phi}{l} \\ -\frac{12}{l^3} & -\frac{6}{l^2} & \frac{12}{l^3} & -\frac{6}{l^2} \\ \frac{6}{l^2} & \frac{2-\phi}{l} & -\frac{6}{l^2} & \frac{4+\phi}{l} \end{bmatrix}, \quad \text{where, } \phi = \frac{12EI}{GSl^2}, \tag{3}$$

where E and G are the elastic modulus and shear elastic modulus, I is the inertia moment to x axis, S is the cross-sectional area, and l is the beam element length. The stiffness matrix K of the shafting can be obtained from the reassembling of the stiffness matrix. The relationship between shafting deformation δ and the load R on it can be expressed by $R = K\delta$. The FEM model of the shafting and the deflection diagram when the displacement value is 0.2 mm is shown in Figure 2.

3.2. Whirling Vibration. The dynamic equation of shafting whirling vibration considering gyroscopic effect is as follows:

$$[\mathbf{M}]\{\ddot{u}\} + ([\mathbf{G}] + [\mathbf{C}])\{\dot{u}\} + ([\mathbf{K}] - [\mathbf{K}_C])\{\mathbf{u}\} = \{\mathbf{F}(t)\}, \tag{4}$$

where [**M**], [**G**], [**C**], [**K**], and [$\mathbf{K}_c$] are the mass, gyroscopic, damping, stiffness matrices, and rotating damping matrix and {**F**} is the external force vector. The gravity, unbalanced force, and the bearing force [24] are included in the exciting matrix $\{\mathbf{F}(t)\}$ as follows:

$$\{\mathbf{F}(t)\} = \mathbf{G} + \mathbf{F}_e + \mathbf{F}_N. \tag{5}$$

The unbalanced force can be expressed as follows:

$$F_e = m_0 e \omega^2. \tag{6}$$

The bearing support force F_N can be obtained by the shafting alignment analysis.

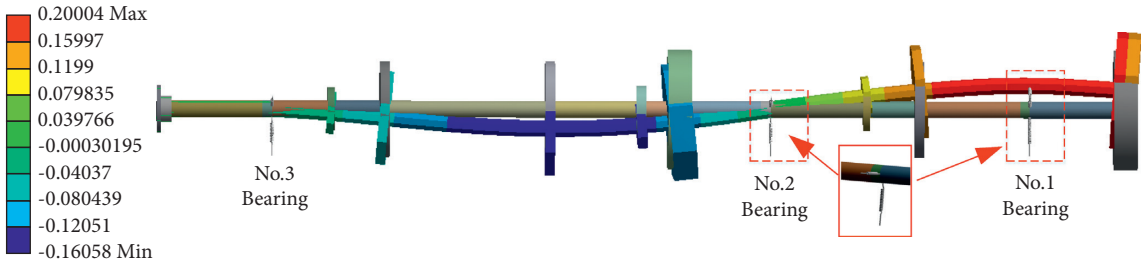

Figure 2: The FEM model and the deflection diagram when the no. 1 bearing offset is 0.2 mm.

The dynamic equation considering the shafting alignment can be expressed as follows:

$$[\mathbf{M}]\{\ddot{u}\} + ([\mathbf{G}] + [\mathbf{C}])\{\dot{u}\} + ([\mathbf{K}] - [\mathbf{K}_C])\{\mathbf{u}\} = \mathbf{G} + \mathbf{m}_0\mathbf{e}\omega^2 + \mathbf{F}_N. \quad (7)$$

3.3. System Analysis and Experiment Design. The shafting system was analysed according to theory of shafting alignment and whirling vibration [25]. The relationship between the load and offset of each bearing is shown in Figure 3 while the angle between the shafting centre line and the No. 1 bearing centre line (ABSB) in each analysis condition is also shown in Figure 3. The load of No. 1 bearing was tested when its offset was 1 mm by using the jacking up method. The tested result shows that the load of No. 1 bearing is 0.38 kN when its offset is 1 mm. Combined with Figure 3, it can be concluded that the actual offset value is about −0.4 mm when the tested offset value of No. 1 bearing is 0 mm. The shafting alignment calculated results will also be used in the analysis of experimental results. The whirling vibration Campbell diagram of the shafting under gravity and bearing support is shown in Figure 4. According to Figure 4, the first- and second-order natural frequencies of the shafting whirling vibration are 46.23 Hz and 59.91 Hz, respectively, which are much higher than the highest rotation frequency of the shafting. This result even does not change when the rotation effect of the shaft and the gyro effect are considered. Thus, the resonance phenomenon is omitted, and only the whirling vibration response is considered.

It can be inferred from Figure 3 that when the offset value of No. 1 bearing is set to 0.2~1.0 mm, the actual bearing offset value is −0.2~0.6 mm. When the test offset value is 0.2 mm, the load distribution of each bearing is the most balanced. So, the test offset value of No. 1 bearing is set to 0.2, 0.4, 0.6, 0.8, and 1.0 mm by setting a standard thickness gasket between the bearing and the base plate. The rotation speed was set to 30 r/min–500 r/min according to the general rotation speed of ship propulsion shafting driven by low-speed engine and middle-speed engines. The Eddy current sensor was chosen to collect the data of the whirling vibration. By comprehensively considering the sensor installation requirements, the measuring point was set at 10 cm after No. 1 bearing. For the convenience of data processing, a hall sensor and a magnet are used to set a phase marker on the axis. The sampling rate is set at 256 Hz. As an important parameter of shafting alignment

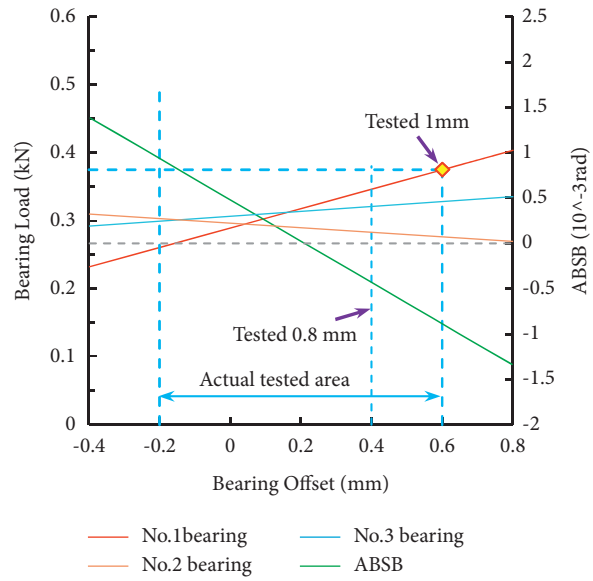

Figure 3: Diagram of shafting alignment and initial state analysis.

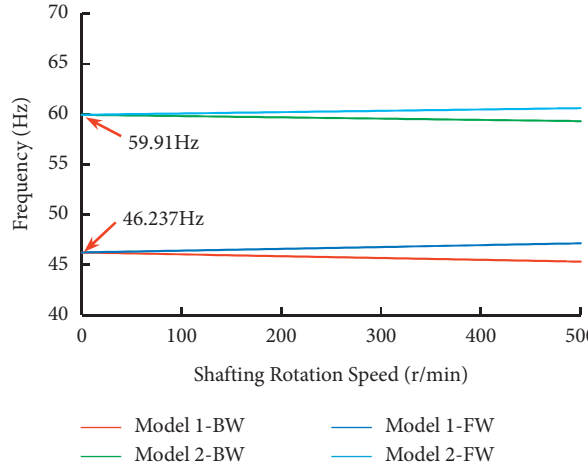

Figure 4: Whirling vibration Campbell diagram.

monitoring, the bearing temperature is tested by using the infrared thermometer. In each operating condition, the bearing temperature is tested for three times, and the average value is taken as the final result. The installation of the sensors is shown in Figure 5.

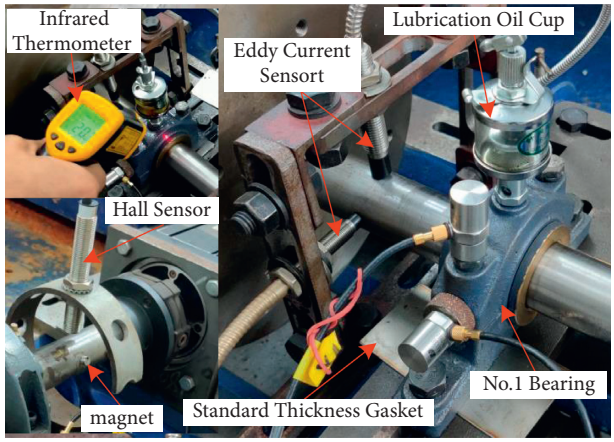

Figure 5: Diagram of sensor installation.

4. Results and Discussion

Two eddy current sensors are installed perpendicularly to obtain the vertical and horizontal vibration data, and 90 s data were collected for each operation condition. Figure 6 shows the collected vibration data in vertical and horizontal direction when the No. 1 bearing offset was 1 mm. The tested data in 5 s are presented.

An obvious 2X harmonic extra peak caused by the vertical bending of shafting in the vertical direction was observed [20]. The time domain waveform feature shows that the shaft was in good consistent with the actual installation of ship shafting.

4.1. Effect on Whirling Vibration Response. Spectral analysis was performed, and the amplitude-frequency diagram when the tested No. 1 bearing offset is 0.8 mm is shown in Figure 7. The frequency of the main peak values was closely related to the rotation speed. As a result, order spectra analysis was adopted. The amplitude-frequency diagram can be converted to the order spectra diagram by periodic sampling by setting the magnet and hall sensor as a cycle marker during the testing. The order spectrum diagram is shown in Figure 8, and the harmonic data are obtained.

As can be seen from Figures 7 and 8, when the tested No. 1 bearing offset is 0.8 mm, the highest amplitude of the 1X harmonic is 1.16×10^{-2} mm in the vertical direction and 1.80×10^{-2} mm in horizontal direction while the highest amplitude of the 2X harmonic is 1.10×10^{-2} mm in the vertical direction and 0.70×10^{-2} mm in horizontal direction. The amplitude of the 1X harmonic was almost equal to 2X harmonic in the vertical direction, which is quite different from the horizontal direction. This is because the shafting system presents a curved state in the vertical direction according to the theory of the reasonable alignment method. The 1X harmonic vibration amplitude in the horizontal direction is much higher than that in the vertical direction.

The values of first 4 harmonic data in the vertical (V) and horizontal (H) ($V/H - n{\cdot}x$) of all cases from the order spectrum are taken for analysis. The peak-peak values (pp) in the time domain of each case are also presented, as shown in Figure 9.

As shown in the peak-peak values in Figure 9, with the rising of No. 1 bearing's location, the whirling vibration peak-peak values in the vertical direction slightly increase. The maximum increment was 7.6×10^{-3} mm from 4.29×10^{-2} mm when the bearing offset was 0.4 mm in 60 r/min to 5.05×10^{-2} mm when the bearing offset was 0.8 mm in 400 r/min. While in the horizontal direction, the increment is 5.38 times larger than that in the horizontal direction. In the horizontal direction, the maximum increment value was 4.09×10^{-2} mm from 4.15×10^{-2} mm when the bearing offset was 0.8 mm in 30 r/min to 8.24×10^{-2} mm when the bearing offset was 1.0 mm in 500 r/min. There was an obvious low amplitude point in each rotation speed condition when the No. 1 bearing offset was 0.8 mm. From the harmonic data in Figure 9, the 1X amplitude contributed the most in the horizontal direction, and the harmonic amplitude decreased at 0.8 mm. This indicated that the shafting whirling vibrational response in the horizontal direction was effectively reduced when the test offset was 0.8 mm without obvious affect in vertical direction. Figure 10 shows the root mean square (RMS) values of whirling vibration changes with the rotation speed in different bearing offset conditions.

In general, the whirling vibration amplitude increases with the increase in rotation speed in both vertical direction and horizontal direction. However, the influence of rotation speed on the amplitude response in the vertical direction was much less than that in the horizontal direction. During the test, the RMS value in the vertical direction is changed from 0.028 mm in 60 r/min when the bearing offset is 0.4 mm to 0.036 mm in 400 r/min when the bearing offset is 1.0 mm with the increase in 0.008 mm. However, the maximum change of RMS value in the horizontal direction is 0.029 mm. When the bearing offset is 0.8 mm, the difference of vibration amplitude in the two directions becomes little and the total vibration is greatly reduced. When the rotation speed was lower than 150 r/min, the amplitude in the vertical direction was almost lower or equal to the amplitude in vertical direction.

4.2. Effect on Axis Movement and Bearing Temperature. Whirling vibration is essentially the vortex around the equilibrium axis position during rotation. And the axis movement state was directly related to the bearing supporting characteristic during the shafting operation. Figure 11(a) shows the axis trajectory in different rotation speeds when the bearing offset was 1 mm. The shafting axis balancing position (SABP) changes with rotation speed can be obtained according to the shafting axis trajectory. Figure 11(a) shows that the shape of the axis trajectory was not much affected by the rotation speed, but the general SABP in the vertical direction changed. The SABP in 30 r/min of each condition is taken as origin point, and the lines of SABP change are presented with rotation speed in the same coordinate, as shown in Figure 11(b).

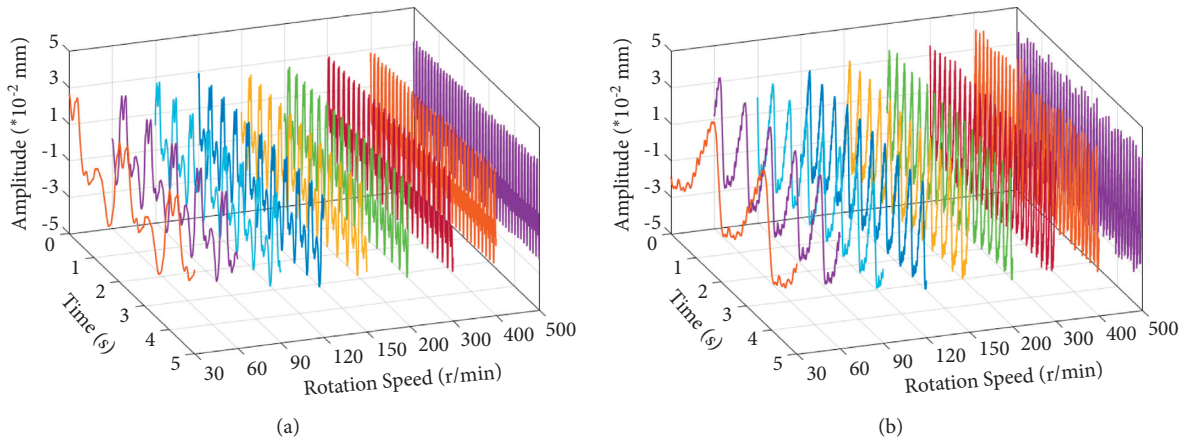

Figure 6: Time domain data of whirling vibration in 200 r/min: (a) vertical and (b) horizontal.

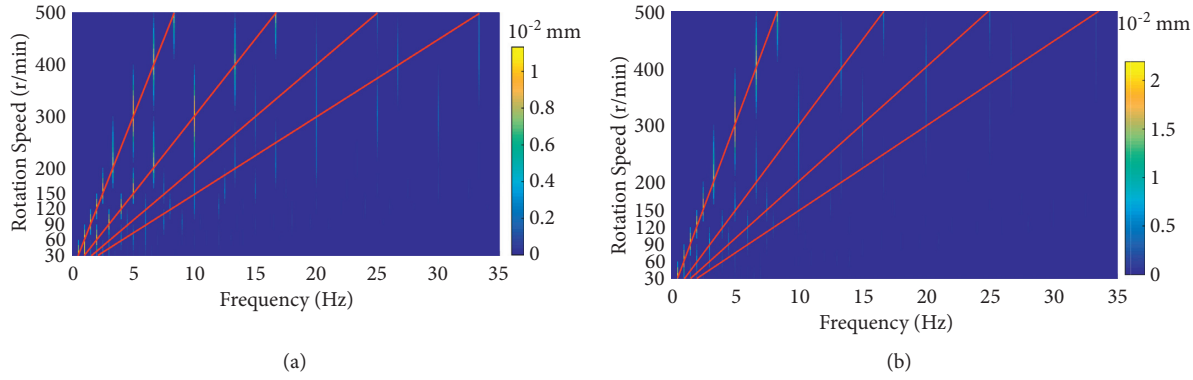

Figure 7: Amplitude-frequency diagram: (a) vertical and (b) horizontal.

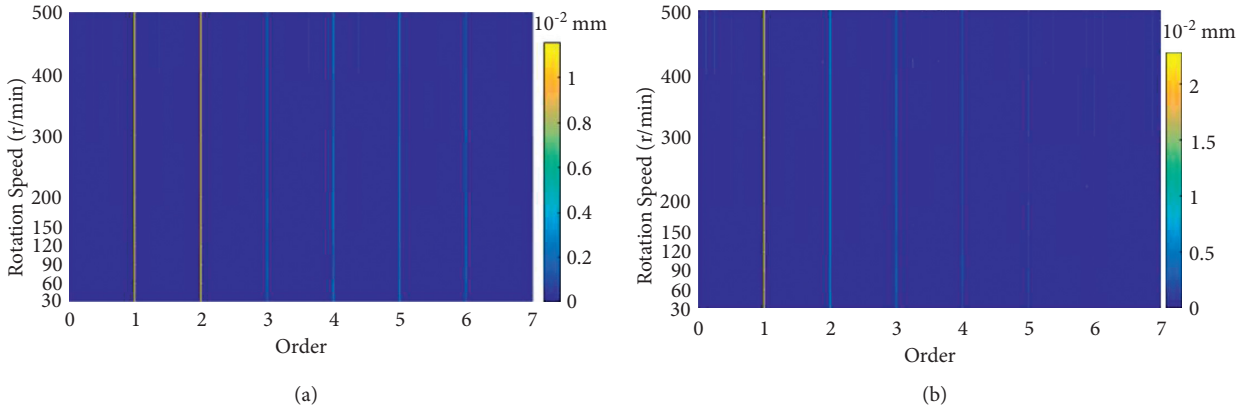

Figure 8: The order spectra diagram: (a) vertical and (b) horizontal.

When the speed is lower than 200 r/min or the bearing offset is 0.6 mm, the SABP is relatively stable. Rotation speed higher than 300 r/min leads to a slightly higher SABP. The maximum upward movement of the SABP is 1.78×10^{-2} mm in 500 r/min when the bearing offset is 0.4 mm. It is due to the increase in the thickness of lubrication oil film with the increase in rotation speed [26]. As the theoretical analysis results of ABSB shown in Figure 3, the ABSB is the smallest when the bearing offset is 0.2 mm (the actual offset is 0.6 mm), with a value of 2.46×10^{-2} rad. The centre line of

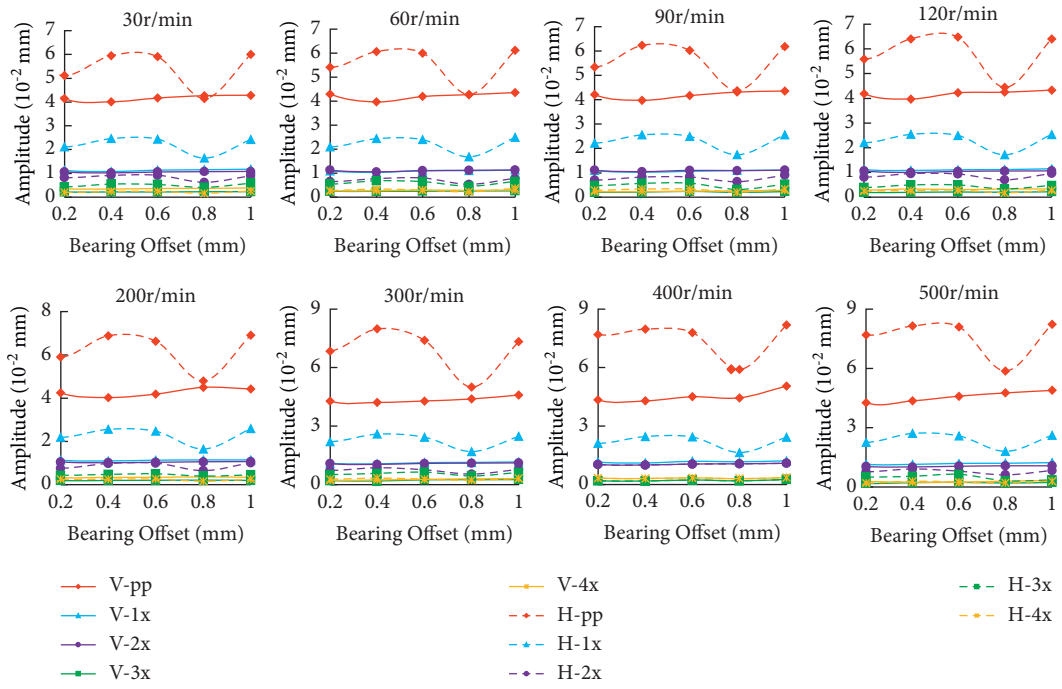

Figure 9: Shafting whirling vibration response with rotation speeds.

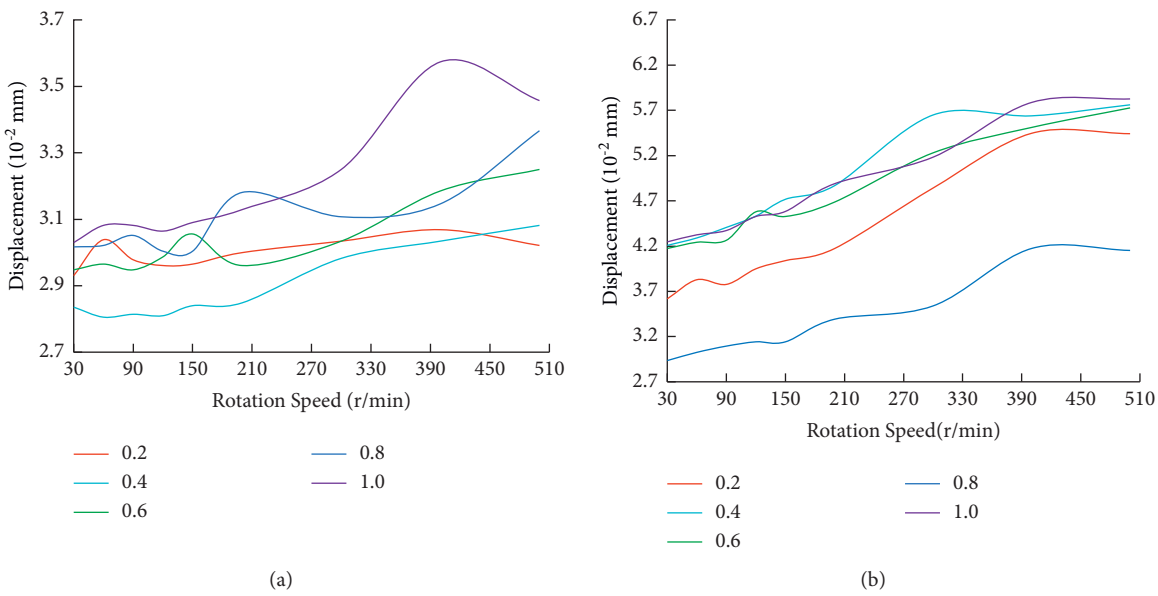

Figure 10: Whirling vibration amplitude changes with rotation speed: (a) vertical and (b) horizontal.

the shafting and the bearing is almost in parallel. The bearing equivalent support position is in the middle of the bearing. The lubrication oil film is the most ideal and stable [27]. Therefore, when the bearing offset is 0.6 mm, the SABP shown in Figure 11(b) is relatively stable. The vertical movement of the shafting leads to load changes of all other bearings on the shafting. Such influence should be considered in the dynamic alignment design of the shafting.

Additionally, the bearing temperature is another important index in the quality evaluation of shafting alignment. It reflects whether the bearing is working normally and whether the shafting state is in good operation condition. The temperature response of No. 1 bearing (BTR) during each condition is shown in Figure 12. The ambient temperature is about 23°C during the whole test.

As shown in Figure 12, the temperature remains the most stable (about 31°C) when the bearing offset is 0.6 mm.

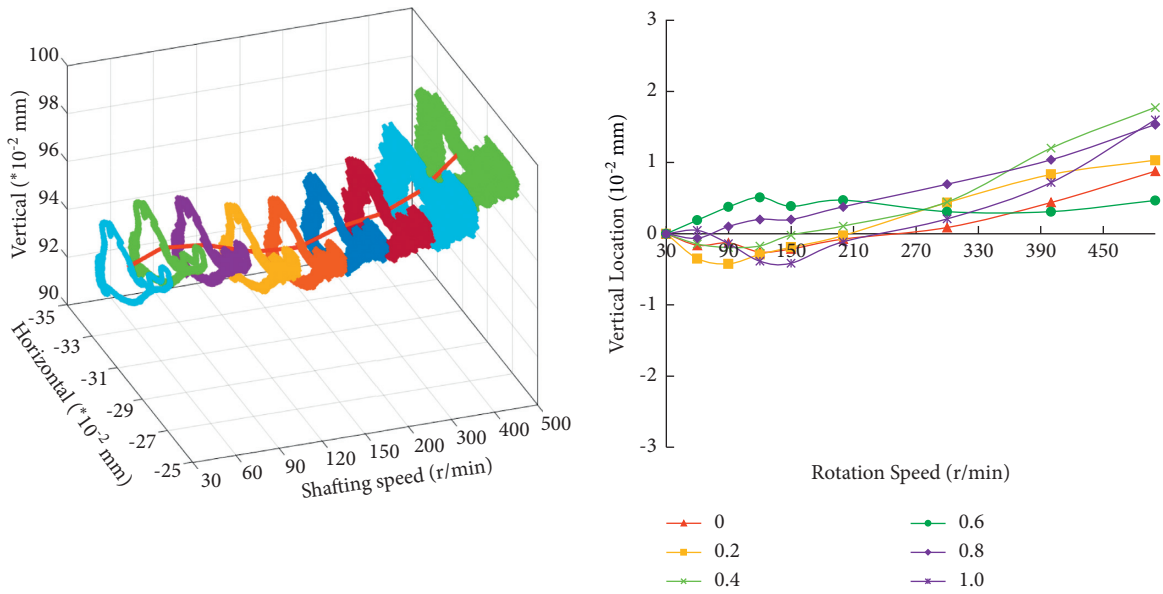

(a) (b)

Figure 11: Axis trajectory and SABP: (a) axis trajectory; (b) SABP change with rotation speed.

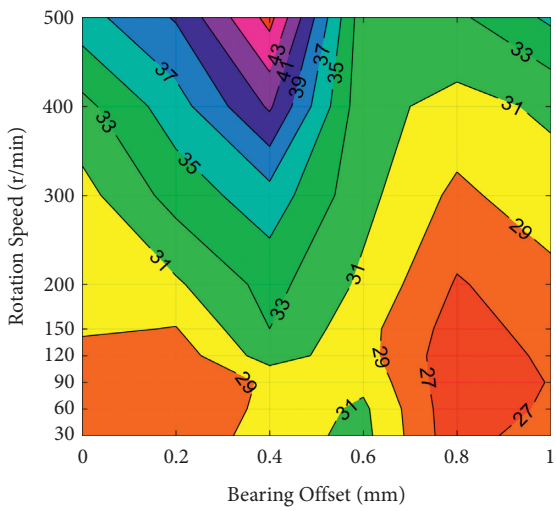

Figure 12: Bearing temperature response.

This feature is completely consistent with the previous data of SABP feature illustrated in Figure 11. This proves that all data are accurate, reliable, and consistent with the analysis results. However, the lowest temperature response appears when the No. 1 bearing offset is 0.8 mm (the calculated offset is 0.6 mm in Figure 3). Combining the results in Figures 9–12, it can be inferred that the best operation state is that the offset of No. 1 bearing which is 0.8 mm. In this condition, both the bearing temperature and the shafting whirling vibration are the lowest. Especially compared with other conditions, it is greatly reduced. The highest temperature appears when the No. 1 bearing offset is 0.4 mm (the calculated offset is 0.6 mm in Figure 3). In this condition, the shafting is in a straight alignment state and the ABSB exists to make the high temperature response. When the bearing offset is lower than 0.4 mm, the temperature response is weaker because of the lower bearing load. When the bearing offset is higher than 0.4 mm, although the bearing load increased, the ABSB decreased and led to the lower temperature. Little ABSB is beneficial to the stable operation of shafting, while appropriately increasing the ABSB and bearing load is beneficial to reducing the shafting whirling vibration. Based on the analysis, it can be inferred that the bearing load and ABSB are the most important factors affecting the whirling vibration and bearing temperature response. By balancing the relationship between bearing load and ABSB, the performance of whirling vibration and bearing temperature response can be optimized.

5. Conclusion

In this work, a reasonable experimental scheme was made according to the theoretical analysis results. The experiment was carried out on the shaft alignment and vibration test rig designed by WUT. The effects of the change of shafting alignment and shafting speed on the whirling vibration and bearing temperature are analysed. The main conclusions of this work are summarized as follows.

Within the shafting designed safe range, the component of whirling vibration in the vertical direction was not clearly affected by the shafting alignment or the rotation speed. The component in the horizontal direction, on the other hand, was clearly affected by both shafting alignment and rotation speed.

The experimental results showed that the horizontal component of the whirling vibration of shafting can be effectively reduced by adjusting the alignment state of shafting. In this case, the amplitude of the whirling vibration response can be reduced.

With an increasing rotation speed, the SABP slightly moved upward after 300 r/min. This leads to load changes of other bearings on the shafting, which should be considered in the dynamic alignment design of the high-speed shafting.

Little ABSB is beneficial to the stable operation of shafting, while appropriately increasing the ABSB and bearing load is beneficial to reducing the shafting whirling vibration.

By balancing the relationship between bearing load and ABSB, the performance of whirling vibration and bearing temperature response can be effectively optimized. The bearing load and ABSB are the most important factors affecting the whirling vibration and bearing temperature response.

Data Availability

The data used to support the findings of this study are available from the corresponding author (Junsong Lei, hbljs0221@163.com) upon request.

Conflicts of Interest

The authors declare that they have no conflicts of interest.

Authors' Contributions

This paper is the result of collaborative teamwork. All authors contributed to the study conception and design. Material preparation, data collection, and analysis were performed by Junsong Lei and Hao Chen. The first draft of the manuscript was written by Junsong Lei. The draft was edited by Junsong Lei, Ruiping Zhou, Yakun Gao, Guobing Huang, and Qingcao Yang. All authors commented on previous versions of the manuscript. All authors read and approved the final manuscript.

Acknowledgments

This work was financially supported by the National Natural Science Foundation of China (51839005) and Major National Science and Technology Projects of China (2017-IV-0006-0043).

References

[1] C. Seo, B. Jeong, J. Kim, and M. Song, "Determining the influence of ship hull deformations caused by draught change on shaft alignment application using FE analysis," *Ocean Engineering*, vol. 210, Article ID 107488, 2020.

[2] Y. Yan, W. Bu, and R. Xu, "The influence of hull deformation on shafting alignment," *Ship Engineering*, vol. 41, pp. 41–44, 2019.

[3] L. Shi, D. Xue, and X. Song, "Research on shafting alignment considering ship hull deformations," *Marine Structures*, vol. 23, no. 1, pp. 103–114, 2010.

[4] L. Murawski, "Shaft line alignment analysis taking ship construction flexibility and deformations into consideration," *Marine Structures*, vol. 18, no. 1, pp. 62–84, 2005.

[5] K. H. Low and S. H. Lim, "Propulsion shaft alignment method and analysis for surface crafts," *Advances in Engineering Software*, vol. 35, no. 1, pp. 45–58, 2004.

[6] M. A. AL-Shudeifat, "New backward whirl phenomena in intact and cracked rotor systems," *Journal of Sound and Vibration*, vol. 443, pp. 124–138, 2019.

[7] Y. Huang, T. Wang, Y. Zhao, and P. Wang, "Effect of axially functionally graded material on whirling frequencies and critical speeds of a spinning Timoshenko beam," *Composite Structures*, vol. 192, pp. 355–367, 2018.

[8] J. S. Sun, T. M. Han, K. K. Lee, and U.-K. Kim, "A study on the measurement and analysis of whirling vibration behavior of marine propulsion shafting system using gap-sensors," *Journal of the Korean Society of Marine Engineering*, vol. 39, no. 2, 2015.

[9] Z. Hui and F. Hai-bao, "Impact of gyroscopic effect on whirling vibration of the ship propulsive shafting," *Ship Engineering*, vol. 36, pp. 74–76, 2014.

[10] T. H. Patel and A. K. Darpe, "Vibration response of a cracked rotor in presence of rotor-stator rub," *Journal of Sound and Vibration*, vol. 317, no. 3-5, pp. 841–865, 2008.

[11] B. Xu, D. Chen, H. Zhang, C. Li, and J. Zhou, "Shaft misalignment induced vibration of a hydraulic turbine generating system considering parametric uncertainties," *Journal of Sound and Vibration*, vol. 435, pp. 74–90, 2018.

[12] Q. Huang, X. Yan, Y. Wang, C. Zhang, and Z. Wang, "Numerical modeling and experimental analysis on coupled torsional-longitudinal vibrations of a ship's propeller shaft," *Ocean Engineering*, vol. 136, pp. 272–282, 2017.

[13] Q. Huang, X. Yan, C. Zhang, and H. Zhu, "Coupled transverse and torsional vibrations of the marine propeller shaft with multiple impact factors," *Ocean Engineering*, vol. 178, pp. 48–58, 2019.

[14] N. Wang and D. Jiang, "Vibration response characteristics of a dual-rotor with unbalance-misalignment coupling faults: theoretical analysis and experimental study," *Mechanism and Machine Theory*, vol. 125, pp. 207–219, 2018.

[15] D. P. Hujare and M. G. Karnik, "Vibration responses of parallel misalignment in Al shaft rotor bearing system with rigid coupling," *Materials Today: Proceedings*, vol. 5, no. 11, pp. 23863–23871, 2018.

[16] F. W. D. S. Tuckmantel and K. L. Cavalca, "Vibration signatures of a rotor-coupling-bearing system under angular misalignment," *Mechanism and Machine Theory*, vol. 133, pp. 559–583, 2019.

[17] N. Sawalhi, S. Ganeriwala, and M. Tóth, "Parallel misalignment modeling and coupling bending stiffness measurement of a rotor-bearing system," *Applied Acoustics*, vol. 144, pp. 124–141, 2019.

[18] Y. Li, Q. Zhou, and D. Wang, "Research on effects of shafting deflection factor for lateral vibration characteristics," *Ship Science and Technology*, vol. 38, pp. 85–91, 2016.

[19] T. H. Patel and A. K. Darpe, "Vibration response of misaligned rotors," *Journal of Sound and Vibration*, vol. 325, no. 3, pp. 609–628, 2009.

[20] C. Y. Z. R. Yang Guodong, "Study on the effects of the different alignment state on shafting vibration," in *Proceedings of the The 21st International Congress on Sound and Vibration*, Beijing, China, July 2014.

[21] G. Lai, J. Liu, S. Liu, F. Zeng, R. Zhou, and J. Lei, "Comprehensive optimization for the alignment quality and whirling vibration damping of a motor drive shafting," *Ocean Engineering*, vol. 157, pp. 26–34, 2018.

[22] G. Lai, J. Lei, J. Liu et al., "Numerical and experimental study on comprehensive optimization for the KPIs of ship propulsion shafting design based on MDO," *Ocean Engineering*, vol. 222, Article ID 108624, 2021.

[23] Z. Yang-Yang and S. Jun, "Research on the influence of shafting alignment condition on transverse vibration transmission characteristics," *Ship Science and Technology*, vol. 42, pp. 65–70, 2020.

[24] B. Ma and Z. Zhang, "Theoretical analysis of the influence of stern bearing elevation on the lateral vibration of shafting," *Noise and Vibration Control*, vol. 35, pp. 56–60, 2015.

[25] J. Lei, R. Zhou, H. Chen, Y. Gao, and G. Lai, "Experimental investigation of effects of ship propulsion shafting alignment on shafting whirling and bearing vibrations," *Journal of Marine Science and Technology*, 2021.

[26] J. Lei, R. Zhou, Y. Sheng, and H. Chen, "Numerical calculation of oil film for ship stern bearing based on matrix method," *MATEC Web of Conferences*, vol. 272, Article ID 1018, 2019.

[27] J. Lei, R. Zhou, H. Chen, and H. Fan, "Research on the effect of aft-stern bearing obliquely boring on bearing performance and shafting transverse vibration," in *Proceedings of the 26th International Congress on Sound and Vibration*, Montreal, QC, Canada, July 2019.